

NASA-CR-172,443

NASA Contractor Report 172443

NASA-CR-172443
19850003788

CHEMOVISCOSITY MODELING FOR THERMOSETTING RESINS - I

FOR REFERENCE

T. H. Hou

NOT TO BE TAKEN FROM THIS ROOM

Kentron International, Inc.
Aerospace Technologies Division
Hampton, Virginia 23666

LIBRARY COPY

NOV 29 1984

Contract NAS1-16000
November 1984

LANGLEY RESEARCH CENTER
LIBRARY, NASA
HAMPTON, VIRGINIA



National Aeronautics and
Space Administration

Langley Research Center
Hampton, Virginia 23665

4 1 1 RN/NASA-CR-172441
5 1 1 RN/NASA-CR-172442
6 1 1 RN/NASA-CR-172443
7 1 1 RN/NASA-CR-172440

DISPLAY 06/2/1

85N12096*# ISSUE 3 PAGE 326 CATEGORY 24 RPT#: NASA-CR-172443 NAS
1.26:172443 CNT#: NAS1-16000 84/11/00 40 PAGES UNCLASSIFIED
DOCUMENT

UTTL: Chemoviscosity modeling for thermosetting resins - I TLSP: Final Report

AUTH: A/HOU, T. H.

CORP: Kentron International, Inc., Hampton, Va. CSS: (Aerospace Technologies
Div.) AVAIL.NTIS SAP: HC A03/MF A01

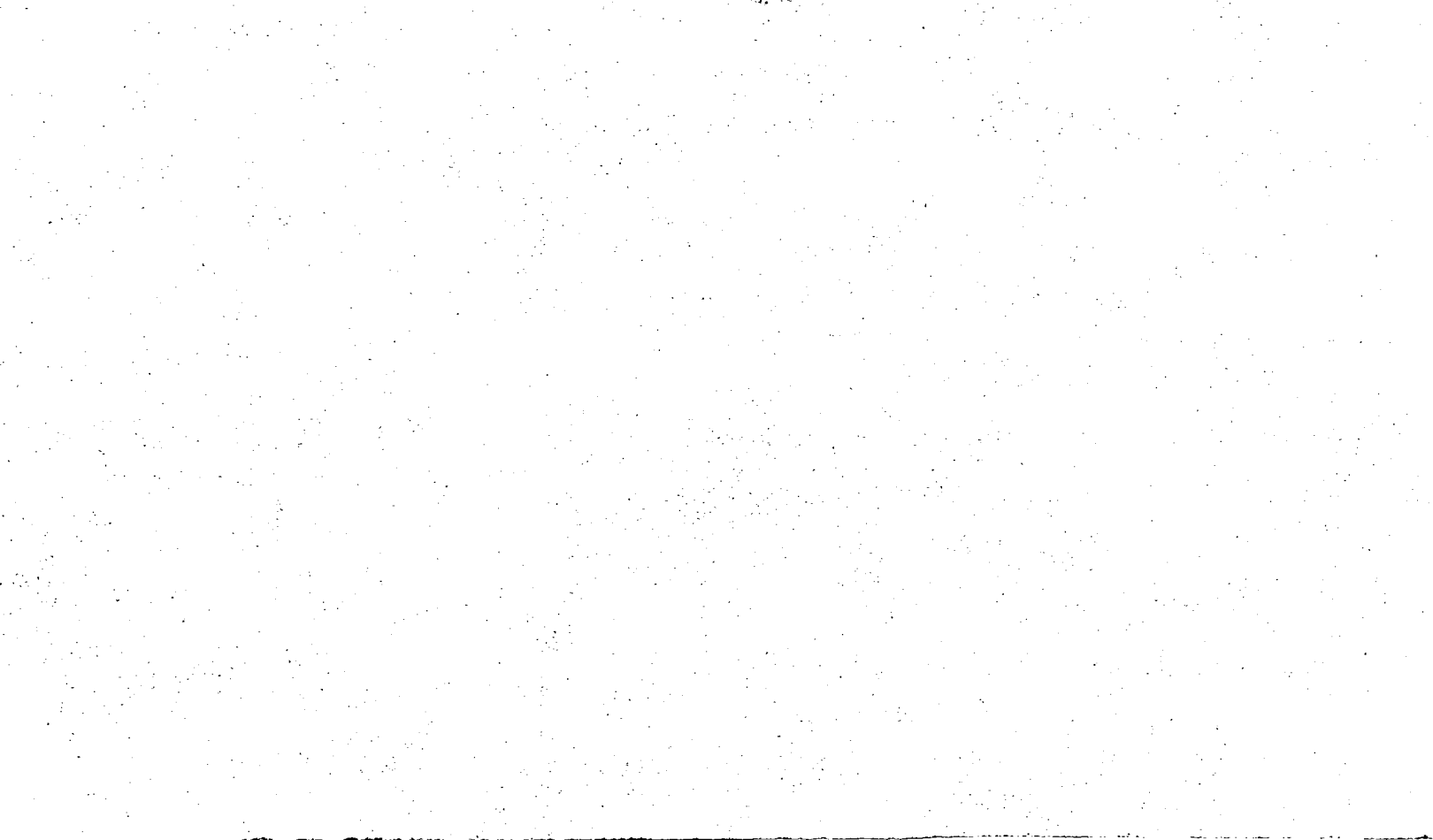
MAJS: /*AUTOCLAVING/*MATHEMATICAL MODELS/*REAL TIME OPERATION/*THERMOSETTING
RESINS

MINS: / CURING/ DIFFUSION/ POLYMERIZATION/ REACTION KINETICS/ RHEOLOGY/
TRANSITION TEMPERATURE/ VISCOSITY

ABA: Author

ABS: A new analytical model for chemoviscosity variation during cure of
thermosetting resins was developed. This model is derived by modifying the
widely used WLF (Williams-Landel-Ferry) Theory in polymer rheology. Major
assumptions involved are that the rate of reaction is diffusion controlled
and is linearly inversely proportional to the viscosity of the medium over
the entire cure cycle. The resultant first order nonlinear differential
equation is solved numerically, and the model predictions compare
favorably with experimental data of EPON 828/Agent U obtained on a
Rheometrics System 4 Rheometer. The model describes chemoviscosity up to a
range of six orders of magnitude under isothermal curing conditions. The

ENTER:



CHEMOVISCOSITY MODELING FOR THERMOSETTING RESINS - I

CONTENTS

	<u>Page</u>
Abstract	ii
Acknowledgement	iii
I. Introduction	1
List of Symbols	3
II. Theory	4
III. Experiment Description	7
IV. Experimental Results	8
V. Model Predictions	9
Isothermal Case	9
Dynamic Heating Case	13
VI. Conclusions	18
References	19
Appendix - Programming Codes	20

ABSTRACT

A new analytical model for chemoviscosity variation during cure of thermosetting resins has been developed. This model is derived by modifying the widely used WLF (Williams-Landel-Ferry) Theory in polymer rheology. Major assumptions involved are that the rate of reaction is diffusion controlled and is linearly inversely proportional to the viscosity of the medium over the entire cure cycle. The resultant first order nonlinear differential equation is solved numerically, and the model predictions compare favorably with experimental data of EPON 828/Agent U obtained on a Rheometrics System 4 Rheometer. It has been shown that the model can describe chemoviscosity up to a range of six orders of magnitude under isothermal curing conditions. The extremely non-linear chemoviscosity profile for a dynamic heating cure cycle can be predicted as well. The model is also shown to predict changes of glass transition temperature for the thermosetting resin during cure. The physical significance of this prediction is unclear at the present time, however, and further research is required. From the chemoviscosity simulation point of view, the technique of establishing an analytical model as described here can easily be applied to any thermosetting resin. The model thus obtained can be used in real-time process controls for fabricating composite materials.

ACKNOWLEDGEMENT

This work, performed at NASA-Langley Research Center (LaRC), was supported by the LaRC Polymeric Materials Branch (PMB) under contract NAS1-16000.

R. M. Baucom (PMB) was the Technical Monitor. Numerous technical consultations with W. T. Freeman (PMB) with regard to the uses of Rheometrics System 4 and HP-9836 computer and helpful discussions with Dr. J. A. Hinkley (PMB) during the course of this work are gratefully acknowledged.

CHEMOVISCOSITY MODELING FOR THERMOSETTING RESINS - I

I. INTRODUCTION

Perhaps the single most important property of a polymer with regard to specifying its processing characteristics is its viscosity, which governs the resin flow characteristics. For thermoplastic materials, the viscosity is influenced by local flow geometry and can vary with temperature and shear rate. Viscosity control becomes more critical and difficult in the processing of thermosetting resins, because of the onset of chemical reactions and the generation of heat during curing which causes the viscosity to vary with time. The term chemoviscosity refers to the variation of viscosity due to polymer chemical reaction. The study of chemoviscosity is generally called chemorheology.¹

In a typical autoclave operation for the fabrication of composite materials,¹ the viscosity-time profile must allow first for the bubbling off of trapped gas, then fiber compaction with resin flow, and, finally, laminate consolidation under applied pressure before the resin has gelled and ceases to flow. At the start of a cure cycle, polymerization begins and the polymer chains lengthen. The increase in viscosity of the resin due to polymerization is, however, largely offset by the increase in temperature which is introduced through the cure cycle and the heat of reaction. Consequently, a drop in resin viscosity of two to three orders of magnitude at the initial stage of cure is not uncommon. As the resin continues to polymerize, crosslinks are formed and the viscosity of the system starts to increase at a faster rate. Finally, the rate of increase of viscosity approaches infinity at gelation. Any chemoviscosity profile is therefore closely related to the reaction kinetics of the resin system and the cure cycle (temperature profile) during processing.

Numerous researchers have devoted considerable efforts to establish an analytical model for the chemoviscosity growth profile of thermosetting resins. The most common approach to this problem has been by empirically specifying the viscosity linearly as an exponential function of reaction time²⁻⁵ or, with the aid of DSC thermal analysis, the degree of cure.⁶⁻⁷ The uses of such relatively simple models were apparently motivated by the empirically observed nearly linear viscosity growth profiles under isothermal cure conditions. A correlation between such isothermal cure model parameters and the curing temperatures can then be established and used to simulate the chemoviscosity growth in a non-isothermal curing condition such as that encountered inside the autoclave. As expected, the nonlinearity of the viscosity-time profile associated with the advancement of resin cure cannot be accounted for satisfactorily by such models.

The objective of this report is to describe the applicability of the well established Williams-Landel-Ferry (WLF) theory in polymer rheology to the chemoviscosity modeling of thermosetting resins. The viscosity-time profiles under both isothermal and dynamic heating conditions are discussed.

LIST OF SYMBOLS

c	Heating rate ($^{\circ}\text{K}/\text{min}$)
C_1, C_2	Constants in WLF Theory, Eq. (1)
C_1^0	Initial value of C_1^i selected for the recursion formula Eq. (6a)
k_0, n_0	Constants for the parameters in Eq. (6b)
$k_{1,2,3,4}$	Parameters defined in fourth-order Runge-Kutta method
k_T	Rate constant of reaction at temperature T
K	$\equiv (dT_g/dT)_{T_g}$
t	Time in minutes
t_f	Time (min) for complete cure of resin
T	Temperature ($^{\circ}\text{K}$) in cure cycle of thermosetting resins
T_0	Starting Temperature ($^{\circ}\text{K}$) of the cure cycle
$T_g(t)$	Glass transition temperature ($^{\circ}\text{K}$) of the thermosetting resin during curing
$\eta_T(t)$	Viscosity (poise) growth of the thermosetting resin during the curing temperature T

II. THEORY

The Williams-Landel-Ferry (WLF) theory⁸ states that for $T_g < T < (T_g + 100^\circ\text{K})$, temperature-dependent viscosity follows the expression:

$$\log \left(\frac{\eta_T}{\eta_{T_g}} \right) = - \frac{C_1(T - T_g)}{C_2 + T - T_g} \quad (1)$$

where C_1 and C_2 are constants. Equation (1) implies that at temperatures above T_g all viscoelastic properties governed by the segmental relaxation rate (e.g., viscous flow, mechanical, and dielectric relaxations, etc.) will vary with temperature in essentially the same way for all polymers. The molecular structure effect on the viscoelastic properties of various polymers will largely disappear when the polymers are compared in corresponding states. The temperature dependency of the viscosity as shown in Equation (1) has been tested and found valid for materials ranging from diluted polymeric systems and thermoplastic melts to rubbers and elastomers.⁹ The equation has also been widely used to describe the time-temperature superpositions for the viscoelastic properties of many thermorheologically simple high polymers.¹⁰ Equation (1) can be derived from the semi-empirical Doolittle equation which relates the viscosity to the free volume of the liquid.¹¹ As the free volume increases, the viscosity rapidly decreases. The two constants C_1 and C_2 are, therefore, related to the fractional free volume at T_g and the thermal coefficient of expansion of the fractional free volume above T_g . C_1 and C_2 were originally thought to be universal constants with values of 17.44 and 51.6 respectively. It was later found that they are material-related. A tabulation of these material constants for various systems can be found in the literature.⁹

The normal use of the WLF equation for thermoplastic materials requires that the glass transition temperature T_g be constant while the temperature T is varied for the specific polymer under study. Eq. (1) is applicable for a temperature T up to 100°K higher than the T_g of the material. However, during cure of thermosetting resins, the monomers are initially polymerized and crosslinks are formed later. This is a system where $T_g(t)$ is changing and the curing temperature T is held constant, in the isothermal case. The glass transition temperature T_g rises continuously and may eventually approach the curing temperature. Over the entire curing cycle, the material structure actually undergoes continuous phase transformations from the low molecular weight liquid to a high molecular weight polymeric melt, and eventually transforms to form crosslinking networks. If it is assumed that $T_g(t)$ of the material is always lower than the cure temperature T , and that $(T-T_g(t))$ is always within 100°K, then the WLF theory should be applicable to all of the different polymer structure phases during cure. Before Equation (1) can be applied to describe the chemoviscosity of the curing resin, however, modifications have to be made in order to account for the time factor. This can be accomplished by the following rationalizations.

It may be assumed that a segmental relaxation rate governs most rate processes that take place in polymers at temperatures above T_g . The rate of reaction is often diffusion controlled, especially in the crosslinking stages. According to the accepted theory of diffusion controlled reactions, the rate constant k_T is generally proportional to the diffusion constant of a reactant, and therefore is inversely proportional to the viscosity of the medium,

$$\frac{\eta_T}{\eta_{T_g}} = \frac{k_{T_g}}{k_T} \quad (2)$$

It is further assumed that the rate constant of reaction k_T is directly proportional to the rate of change of the glass transition temperature T_g ,

$$\frac{k_T}{k_T} = \left(\frac{dT_g}{dt}\right)_{T_g} / \left(\frac{dT_g}{dt}\right)_T \quad (3)$$

Equations (1), (2), and (3) can then be combined to form a first order ordinary nonlinear differential equation:

$$\left(\frac{dT_g}{dt}\right)_T = K \exp \left[\frac{C_1(T-T_g)}{C_2+T-T_g} \right] \quad (4)$$

where $K = (dT_g/dt)_{T_g}$ is the rate of change of T_g at $T = T_g$, and is taken to be a material constant.

With the boundary condition that as $t \rightarrow t_f$, $T_g \rightarrow T$ where t_f denotes the time for complete cure of the resin and T denotes the cure temperature, Equation (4) can be solved numerically for T_g as a function of curing time, t . The chemoviscosity of the curing resin can then be obtained by Equation (1).

In the case of dynamic heating curing conditions, T in Equation (4) can be replaced by $(T_0 + ct)$, where T_0 is the starting temperature and c is the heating rate in ($^{\circ}\text{C}/\text{min}$). For a given cure cycle (i.e., temperature profile inside the autoclave), two material constants, η_{T_g} and $(dT_g/dt)_{T_g}$, and the two WLF constants C_1 and C_2 need to be specified before Equations (4) and (1) can be solved. Details for solving these equations will be discussed in Section V.

III. EXPERIMENT DESCRIPTION

A diglycidyl ether of bisphenol A based epoxy resin EPON 828 (Shell) was studied. The hardener selected was a liquid amine EPON Curing Agent U, also from Shell. EPON 828 and Agent U were weighed separately with a microbalance which has a resolution of 0.001 gm. A weight ratio of 100/25 was studied. The two components were hand mixed for 2 minutes before being transferred to a Rheometrics System 4 Rheometer for chemoviscosity measurements.

The sample was confined in the gap between two parallel plates mounted in the Rheometer. The top plate is motor driven about its axis while the bottom plate is mounted on a torque transducer for force measurement. The typical gap between the parallel plates was 1.2 mm. The plates and sample are enclosed in a heat chamber where temperature control is provided. Though the shear field in parallel-plate flow geometry is non-uniform, for the small amplitude displacements used, these effects can be safely neglected. Plate oscillatory motion was set at a frequency of 10 rad/sec, and an amplitude (strain) equivalent of 1 percent of the gap was used for all measurements reported. Selection of the strain value was to assure that the measurements were performed within the material's linear viscoelastic response range.

It is well known that the viscoelastic properties of polymeric materials respond differently to different frequencies, and selection of the frequency value was made to assure that the complex viscosities measured were within the Newtonian region.¹² The cure mode of the Rheometer was used during testing which automatically programs different temperature profiles as the epoxy is cured. Both isothermal and dynamic heating measurements were performed.

IV. EXPERIMENTAL RESULTS

Chemoviscosity increase profiles for isothermal curing at three different temperatures are shown in Figure 1. The first data point, measured at $t = 0$, corresponds to approximately 5 ± 0.5 minutes delay from the beginning of sample mixing in all cases. The initial viscosity is lower when the material is cured at higher temperatures. This is believed to be due to the temperature effect. Figure 1 shows the nonlinearity in the viscosity-time profiles, especially during the initial stages of cure. The profiles become more linear as cure progresses. From the process point of view, the initial stages of cure are far more important because the resin flow is easier to control. A linear chemoviscosity model in this region would certainly be inadequate.

The chemoviscosity profile for a dynamic heating condition is shown in Figure 2. The temperature profile is also included in the figure. The sample is first heated at a rate of $1^{\circ}\text{C}/\text{min}$ from 32°C to 62°C , then the temperature remains constant throughout the cure cycle. The viscosity initially decreases and then increases exponentially. Such viscosity profiles are typical for thermosetting resins under dynamic heating conditions. The decrease in viscosity during the heat up period provides more flexibility in resin flow adjustments for the fabrication of composite materials in an autoclave. Precise chemoviscosity modeling is therefore more important under these conditions.

V. MODEL PREDICTIONS

Isothermal case

Using Equation (4), which is rewritten here,

$$\left(\frac{dT_g}{dt}\right)_T = K \exp \left[\frac{C_1(T-T_g)}{C_2+T-T_g} \right] \quad (4)$$

the glass transition temperature $T_g(t)$ can be obtained. The chemoviscosity of the curing resin can then be calculated by

$$\begin{aligned} \eta_T(t) &= \eta_{T_g} \exp \left[\frac{-C_1(T-T_g)}{C_2+T-T_g} \right] \\ &= (\eta_{T_g} \cdot K) / (dT_g/dt) \end{aligned} \quad (5)$$

The two material constants K and η_{T_g} have been assigned values of $2 \times 10^{-7} \text{ }^\circ\text{K/min}$ and $1 \times 10^8 \text{ poise}$, respectively, for all the isothermal model predictions described below. Physically, these two material constants represent the material properties of the resin at the completely cured state.

Constant C_1 in the WLF theory is assumed as a function of T_g by the following recursion formula

$$C_1^{i+1} = C_1^i (T_g^i / T_g^{i+1})^n$$

with

$$T_g^i(t) = T_g(i\Delta t), \quad i = 0, 1, 2, \dots$$

(6a)

and

$$n = n_0 e^{k_0 t} \quad (6b)$$

while C_2 is assigned the "universal constant" of 51.6°K. The change of C_1 as the resin curing progresses (Eq. (6a)) is required by noting that values of C_1 vary for different polymeric systems ranging from dilute solutions to cross linked rubbers.⁹

The initial condition, $T_g(0)$ at $t = 0$, is difficult to specify but is required in order to solve the differential Equation (4). Theoretically, $T_g(t_f)$ should be equal to the cure temperature T when the time t_f for the completely cured stage is reached. However, in practice t_f may well approach infinity. In the present study, $T_g(0)$ is arbitrarily chosen, and the simulated results for $T_g(t)$ that were obtained can only describe the relative changes of T_g as a function of time for the resin under study.

The constants used to solve Equations (4), (5), and (6a,b) for the isothermal curing of the EPON 828/Agent U system with weight ratio of 100/25 reported here are summarized in Table 1.

TABLE 1. Constants used in the theory for isothermal case.
(EPON 828/Agent U, 100/25 weight ratio)

Cure Temp. T (°K)	$T_g(0)$ (°K)	K (°C/min)	η_{T_g} (poise)	C_1^0	C_2	n_0	k_0
305	280	$2 \cdot 10^{-7}$	$1 \cdot 10^8$	41.5	51.6	1	0.165
310	280	$2 \cdot 10^{-7}$	$1 \cdot 10^8$	38	51.6	1	0.245
317	280	$2 \cdot 10^{-7}$	$1 \cdot 10^8$	37	51.6	1	0.385

Equation (4) is solved numerically by a fourth-order Runge-Kutta method¹³ as modified by Gill:

$$T_g^{i+1} = T_g^i + \frac{h}{6} \left[k_1 + 2\left(1 - \frac{1}{\sqrt{2}}\right) k_2 + 2\left(1 + \frac{1}{\sqrt{2}}\right) k_3 + k_4 \right]$$

$$k_1 = f(t^i, T_g^i)$$

$$k_2 = f\left(t^i + \frac{h}{2}, T_g^i + \frac{h}{2} k_1\right)$$

(7)

$$k_3 = f\left(t^i + \frac{h}{2}, T_g^i + \left(-\frac{1}{2} + \frac{1}{\sqrt{2}}\right)hk_1 + \left(1 - \frac{1}{\sqrt{2}}\right)hk_2\right)$$

$$k_4 = f\left(t^i + h, T_g^i - \frac{1}{\sqrt{2}}hk_2 + \left(1 + \frac{1}{\sqrt{2}}\right)hk_3\right)$$

where h is the time increment and

$$f(t, T_g) = K \exp \left[\frac{C_1(T - T_g)}{C_2 + T - T_g} \right] \quad (8)$$

This algorithm was programmed in Basic and solved on a Hewlett-Packard HP-9836 computer. The program listing is included in the Appendix for reference.

Numerical solutions are plotted in Figure 1 with the experimental data for isothermal curing at three temperatures. Good agreement between the data and theory for all three cases are noted. The capability of the model to describe up to six orders of magnitude in chemoviscosity range is significant. Numerical computations were performed for different time increment (Δt and h in Eq. (6a) and (7), respectively). It was found that the simulated chemoviscosities based on $\Delta t = 0.5$ and 0.25 minutes, respectively, differ by less than 1% for all three temperatures. The simulated initial viscosities for various temperatures are the result of different assigned values of C_1^0 and n_0 , while the simulated viscosity increase rates are dictated by the assigned k_0 . Variations of the computed C_1 are plotted in Figure 3. It is noted in the literature⁹ that C_1 varies from 11.2 for polybutadiene rubber to 34.0 for Methyl (atactic) polymer. The variations of C_1 shown dictate structure changes of the material under investigation, and are approximately equivalent to a variation from 0.011 to 0.087 for f_g , the fractional free volume at T_g , of the curing resin.

Calculated values for $T_g(t)$ for the curing resin are also shown in Figure 3. It can be noted that changes of T_g are faster for higher cure temperatures during early curing stages. Higher cure temperatures yield higher T_g . After the initial curing period of approximately 20 minutes, values of T_g quickly level off; the chemoviscosities $\eta(t)$, however, keep increasing as can be seen from Figure 1. Similar situations exist in the relationship between $\eta(t)$ and $\alpha(t)$, the degree of cure determined by DSC thermal analysis, as reported experimentally by Lee et al.⁷ These observations imply that determinations of gelation points of the thermosetting resins by viscosity data alone are questionable. Further research in this area is planned. $T_g(t)$ in Figure 3 increases very slowly after the initial 20 minutes, and may take a very long time

to reach cure temperatures of 305, 310, and 317°K, respectively. This is in agreement with the fact that low curing temperatures are employed.

The analytical model developed here (i.e., Eqs. (4), (5), and (6a,b)) possesses three material constants and four adjustable parameters. In describing the chemoviscosity under isothermal curing, however, only two parameters (C_1^0 and k_0 in Table 1) need to be adjusted in order to account for the differences in cure temperatures. It can be noted from Figure 1 that the model predictions are in better agreement with the experimental data than the empirical 4-parameter model used in the literature³. The values of C_1^0 and k_0 used follow the Arrhenius relationship shown in Figure 4. The Arrhenius correlation makes chemoviscosity predictions possible for this material at temperatures outside the range studied here.

Dynamic Heating Case

In this case cure temperature changes with time. The value of T in Equations (4) and (5) is replaced by $(T_0 + ct)$, where T_0 is the start temperature and c is the rate of increase of the temperature. Equation (4) becomes

$$\frac{dT_g}{dt} = K \exp \left[\frac{C_1(T_0 + ct - T_g)}{C_2 + T_0 + ct - T_g} \right] \quad (9)$$

When Equation (9) is directly applied to the cure cycle shown in Figure 2 using the material constants listed in Table 1, the predictions as plotted by the dashed line are relatively poor. The drop in viscosity in the initial cure portion is overestimated, and the rate of viscosity increase as the cure

progresses is not as high as those experimentally measured. By selecting the following new set of constants: $K = 9.2 \times 10^{-7}$, $C_1^0 = 41.0$ and

$$\begin{array}{lll} n_0 = 1, & k_0 = 0, & \text{for } 0 < t < 15 \text{ mins} \\ & = 0.00012, & = 0.62, & 15 < t < 21 \\ & = 0.00012, & = 0.59, & 21 < t \end{array}$$

the simulated results shown by solid line in Figure 2 are in very close agreement with the experimental data.

When numerical computations were performed for two different time increments ($\Delta t = 0.5$ and 0.25), the values of calculated chemoviscosity differed by less than 1%. The variations of $T_g(t)$ and $C_1(t)$ during cure are shown in Figure 5. The behaviors of T_g and C_1 are very similar to those discussed before under isothermal cure cases.

The theory was also compared with dynamic heating cure data reported by Tajima and Crozier.¹ The material used was composed of two epoxy resins, TGMMA-MY720 of 69 wt. percent and SU-8 of 9 wt. percent, and an amine hardener DDS of 22 wt. percent. The cure cycle for this resin together with the chemoviscosity data are reproduced in Figure 6. Material constants selected for the model are as follows:

$$T_g(0) = 284^\circ\text{K}, K = 2 \cdot 10^{-10} \text{ }^\circ\text{K}/\text{min}$$

$$\eta_{T_g} = 1 \times 10^{10} \text{ poises}, C_1^0 = 31.6, C_2 = 51.6^\circ\text{K}$$

$$n_0 = 0.1, \quad k_0 = .001, \quad \text{for} \quad 0 < t < 71 \text{ min}$$

$$= 0.0002, \quad = 0.1, \quad 71 < t < 111$$

$$= 4 \times 10^{-5}, \quad = 0.1, \quad 111 < t < 121$$

$$= 1 \times 10^{-5}, \quad = 0.115, \quad t > 121$$

Excellent agreement was demonstrated between the model predictions and experimental data. Variations of $T_g(t)$ and $C_1(t)$ during cure are also plotted in Figure 7. The behaviors of these quantities are similar to those discussed before for the Epon 828/Agent U system.

Equations (6a) and (6b) have been incorporated in Equation (4) or (9) to simulate the chemoviscosity of thermosetting resins under various cure cycles discussed so far. Equations (6a) and (6b) are, however, purely empirical. Other forms can also be successfully used. For example, consider the following new equation:

$$C_1 = C_1^0 \left[1 + \log\left(\frac{T_g}{T}\right)^{k_0} \right] \quad (10a)$$

and the recursion formula for k_0 as

$$k_0^{i+1} = k_0^i \times (T_g^{i+1}/T_g^i) \times n_0 \quad (10b)$$

Material constants selected for this model are as follows:

$$T_g(o) = 46^\circ\text{K}, K = 5 \times 10^{-14} \text{ }^\circ\text{K/min}$$

$$\eta_{T_g} = 1 \cdot 10^{13} \text{ poises, } C_1^0 = 32.44, C_2 = 51.6^\circ\text{K}$$

while

$$\begin{array}{lll} n_o = 0.98, & k_o^0 = 0.19, & \text{for } 0 < t < 75 \text{ min} \\ & = 1.025, & = 0.19, \quad 75 < t < 111 \\ & = 1.008, & = 0.19, \quad t > 111 \end{array}$$

When the temperature profile in Figure 8 is followed, Equations (9), (10a), and (10b) give solutions plotted as the solid curve in Figure 8. The model predictions again agree well with the experimental data over the entire cure cycle.

Tajima and Crozier¹ used the same WLF Theory to explain their experimental data. However, the treatments are quite different from those described in this paper. They choose reference temperatures $T_s(t)$ to replace $T_g(t)$ in Eq. (1). While both $\eta_{T_s}(t)$ and $T_s(t)$ are varied, the constants C_1 and C_2 are kept constant during the entire cure cycle. The values of $\eta_{T_s}(t)$ and $T_s(t)$ are related to the content of unreacted curing agent (DDS) where the time factor is introduced. Physically, continuous changes of reference viscosity and temperature in the WLF theory imply continuous changes in molecular structures of the material. This accounts for the good agreement between their model and the

experimental data. The approach reported in this paper involves only one experiment (i.e. Rheometry) and the model is much easier to establish.

Mussatti and Macosko¹⁴ reported steady shear viscosity data on EPON 828 catalyzed by 1% by weight of triethanolamine (TEA) under isothermal curing at 100°C. Viscosity measurements were made with cone and plate flow geometry of a Rheometrics Mechanical Spectrometer. Rotation was started and stopped periodically as the reaction proceeded, and the resulting torque was recorded until the sample broke up. The viscosity data obtained in this experiment are reproduced in Figure 9. Attempts have also been made to fit the data with the model, i.e., Eqs. (10a,b) for the parameters C_1 and k_0 have been used together with the model Eq. (4). Material constants and parameters selected for the model are as follows:

$$T_g(0) = 150^\circ\text{K}, K = 5.0 \times 10^{-14} \text{ }^\circ\text{K/min}$$

$$\eta_{Tg} = 1 \times 10^{13} \text{ poises}, C_1^0 = 38.44, C_2 = 51.6^\circ\text{K}$$

and

$$\eta_0 = 1.01, k_0 = 0.1, \text{ for } 0 < t < 50 \text{ mins}$$

$$= 1.045, \quad = 0.1 \quad 50 < t < 60$$

$$= 1.022, \quad = 0.1 \quad t > 60$$

It can be seen in Figure 9 that the theory can also describe the steady shear viscosity data very well. Variations of $T_g(t)$ and $C_1(t)$ during cure are plotted in Figure 10 for reference. The behaviors of these quantities are again similar to those discussed before for other resin systems.

VI. CONCLUSIONS

It has been shown that the WLF theory, Equations (4) and (9), with the appropriately selected material constants can accurately predict the chemoviscosity of thermosetting resins. The success in applying the theory to an entire cure cycle for both isothermal and dynamic heating conditions indicate valid assumptions for chemoviscosity model development. It is surprising to note that the simple assumption of Eq. (2) (where viscosity is assumed to be linearly inversely proportional to the rate constant of reaction) incorporated with WLF theory can account for the chemoviscosity increase over an entire cure cycle. The demonstrated capability to describe up to six orders of magnitude of change in the chemoviscosity range with the model is significant. The model can also predict the change of glass transition temperature $T_g(t)$ during cure. The physical significance of the predicted $T_g(t)$ which results from the assumption of Eq. (3) in the theory is unclear at the present time. A thorough understanding of the kinetics of chemoviscosity, the degree of cure, the stoichiometry and mechanism of polymerization can only be achieved by a combined use of several analytical methods, such as Rheometry, DSC, TBA, and spectroscopy. Such tasks remain to be resolved in the future.

The model as described has considerable value in autoclave process monitoring applications. An analytical model with the appropriate parameters determined from a single set of experimental data (e.g., via Rheometry) can easily be established for any thermosetting resin. The established model, which has the capability of describing the chemoviscosity accurately, can be used in real-time control of automatic composite processing equipment when an appropriate sensing device can be identified.

REFERENCES

1. Tajima, Y. A.; and Crozier, D.: "Thermokinetic Modeling of an Epoxy Resin I. Chemoviscosity," *Polym. Engr. Sci.*, 23, 186, 1983.
2. Roller, M. B.: "Characterization of the Time-Temperature-Viscosity Behavior of Curing B-Staged Epoxy Resin," *Poly. Engr. Sci.*, 15, 406, 1975.
3. Carpenter, J. F.: "Processing Science for AS/3501-6 Carbon/Epoxy Composites," Technical Report N00019-81-C-0184, McDonnell Aircraft Co., 1983.
4. Kamal, M. R.; Sourour, S.; and Ryan, M.: "Integrated Thermo-Rheological Analysis of the Cure of Thermosets," Technical Papers, 31st Annual Technical Conference, SPE, 187, 1973.
5. Kamal, M. R.: "Thermoset Characterization for Moldability Analysis," *Polym. Engr. Sci.*, 14, 231, 1974.
6. Stolin, A. M.; Merzhanov, A. G.; and Malkin, A. Y.: "Non-Isothermal Phenomena in Polymer Engineering and Science: A Review. Part II: Non-Isothermal Phenomena in Polymer Deformation," *Polym. Engr. Sci.*, 19, 1065, 1979.
7. Lee, W. I.; Loos, A. C.; and Springer, G. S.: "Heat of Reaction, Degree of Cure, and Viscosity of Hercules 3501-6 Resin," *J. Compo. Matl.*, 16, 510, 1982.
8. Williams, M. L.; Landel, R. F.; and Ferry, J. D.: "The Temperature Dependence of Relaxation Mechanisms in Amorphous Polymers and Other Glass-forming Liquids," *J. Amer. Chem. Soc.*, 77, 3701, 1955.
9. Ferry, J. D.: "Viscoelastic Properties of Polymers," 2nd ed., pp. 316, John Wiley & Sons, Inc., 1970.
10. Kaniskin, V. A.; Kaya, A.; Ling, A.; and Shen, M.: "Mechanical and Dielectric Relaxations in Alternating Block Copolymers of Dimethylsiloxane and Bisphenol A Carbonate," *J. Appl. Polym. Sci.*, 17, 2695, 1973.

11. Aklonis, J. J.; MacKnight, W. J.; and Shen, M.: "Introduction to Polymer Viscoelasticity," pp. 53, John Wiley & Sons, Inc., 1972.
12. Bird, R. B.; Armstrong, R. C.; and Hassager, O.: "Dynamics of Polymeric Liquids, Vol. 1," pp. 194, 1977.
13. Carnahan, B.; Luther, K. A; and Wilkes, O. J.: "Applied Numerical Methods," pp. 363, John Wiley & Sons, Inc., 1969.
14. Mussatti, F. G.; and Macosko, C. W.: "Rheology of Network Forming Systems," Polym. Engr. Sci. 13, 236, 1973.

APPENDIX

Shown herein is a listing for solving Eqs. (4), (5), (6a,b) by means of a Runge-Kutta algorithm. Hewlett-Packard Basic Extension 2.0 language is used. The program is run on a HP-9836 computer.

```

10 ! 2/8/84. "DIFFER3_A0"
20 ! 2/15/84. REVISED 1 TO ACCOMMODATE BOTH CONST AND NONISO-THERMAL CASES
30 !
40 ! THIS PROGRAM FIXES FINAL CURING TEMP = T AT TIME=TFINAL
50 ! ADJUSTABLE VARIABLES ARE K,A,B FOR THE NON-ISOTHERMAL CASE
60 ! NUMERICAL SOLUTIONS ARE PROVIDED BY SHOOTING METHOD IN-
70 ! CORPORATED WITH THE RUNGE-KUTTA 4TH ORDER SCHEME TO SOLVE
80 ! THE DIFFERENTIAL EQUATION
90 ! IT HAS BEEN ASSUMED THAT  $K=(DTG/DT)$  AT TG IS A CONSTANT;
100 ! THAT  $A(I)=A0(I)*(TG(I)/TG(I+1))^N$ ,  $A(I)=C1$ 
110 !  $B=51.6$ ,  $B=C2$  IN WLF THEORY
120 ! .....CONST AND NON-ISOTHERMAL CASE .....
130 !
140 COM Timechg0,Timechg1,Timechg2,Timechg3,Cc,A0
150 COM Tg0temp,Tg0last,Tg0now,Alast,Anow
160 COM Nn,N0,N1,N2,N3,Kn1,Kn2,Kn3,Kn4,Kn5,Kn6,Kn7,Kn8
170 !
180 Tg0=284
190 K=2.0E-10
200 A0=31.6
210 N0=.1
220 Kn2=.001
230 Timechg0=71
240 !
250 N1=.0002
260 Kn4=.1
270 Timechg1=111
280 !
290 N2=.00004
300 Kn6=.1
310 Timechg2=121
320 !
330 N3=.00001
340 Kn8=.115
350 Timechg3=2000
360 !
370 LET A=A0
380 LET B=51.6
390 C1st=1.
400 C2nd=.8
410 Time1=70
420 Time2=115
430 Tstart=338
440 Temp=Tstart
450 Tfinal=1000
460 Xxtg=1.E+10
470 !
480 H=.5
490 !
500 PRINT "DIFFER3_A0_CROZIER2"
510 PRINT
520 PRINT "SOLUTIONS FOR TSTART(K)=";Tstart;" TFINAL(MIN)=";Tfinal
530 PRINT "A0=";A0;"B=";B;"K=";K;"H=";H
540 PRINT "TEMP PROFILE IS C1ST=";C1st;" AT TIME1=";Time1
550 PRINT " AND C2ND=";C2nd;" AT TIME2=";Time2
560 PRINT "TIMECHG0=";Timechg0;"N0=";N0;"KN1=";Kn1;"KN2=";Kn2
570 PRINT "TIMECHG1=";Timechg1;"N1=";N1;"KN3=";Kn3;"KN4=";Kn4
580 PRINT "TIMECHG2=";Timechg2;"N2=";N2;"KN5=";Kn5;"KN6=";Kn6
590 PRINT "TIMECHG3=";Timechg3;"N3=";N3;"KN7=";Kn7;"KN8=";Kn8
600 PRINT "XXTG=";Xxtg
610 PRINT

```

```

620 !
630 Time0=0.
640 Clock=1
650 Dtgdt=FNValue(Time0.Tg0.A.B.Time0.K.Tstart.Tstart)
660 Xx=Xtg*K/Dtgdt
670 PRINT Time0.Tg0." ".Dtgdt."XX=".Xx
680 PRINT
690 ! TEMPERATURE PROFILE IS DEFINED AS FOLLOWS:
700     IF Time0<Time1 THEN
710         Cc=C1st
720         Temp=Tstart+Cc*Time0
730         Tempnow=Tstart+Cc*(Time0+H)
740         GOTO 880
750     ELSE
760         GOTO 770
770     END IF
780     IF Time0<Time2 THEN
790         Cc=0
800         Temp=Tempnow
810         Tempnow1=Temp
820         GOTO 880
830     ELSE
840         Cc=C2nd
850         Temp=Tempnow1+C2nd*(Time0-Time2)
860         Tempnow=Tempnow1+Cc*(Time0+H-Time2)
870     END IF
880 CALL Runge_kutta(Time0.Tg0.H.Tgnew.A.B.Time0.K.Tstart.Temp)
890 Tg0=Tgnew
900 Tg0last=Tg0temp
910 Tg0now=Tg0
920 Alast=Anow
930 Timenow=Time0+H
940 Dtgdt=FNVal0(Anow.B.Timenow.Tg0.K.Tempnow)
950 Xx=Xtg*K/Dtgdt
960     IF Timenow>Tfinal THEN
970         GOTO 1100
980     ELSE
990         GOTO 1010
1000    END IF
1010    IF Timenow=Clock THEN
1020        Clock=Clock+5
1030        PRINT Timenow;Tempnow;Tg0;Dtgdt:"XX=":Xx;Anow
1040        Time0=Time0+H
1050        GOTO 700
1060    ELSE
1070        Time0=Time0+H
1080        GOTO 700
1090    END IF
1100 END
1110 !
1120 !
1130 SUB Runge_kutta(X1.Y1.H.Y11.A.B.Time.K.Tstart.Temp)
1140 COM Timechg0,Timechg1,Timechg2,Timechg3.Cc.A0
1150 COM Tg0temp,Tg0last,Tg0now,Alast,Anow
1160 COM Nn,N0,N1,N2,N3,Kn1,Kn2,Kn3,Kn4,Kn5,Kn6,Kn7,Kn8
1170 Tg0temp=Y1
1180 K1=FNValue(X1.Y1.A.B.Time.K.Tstart.Temp)
1190 Xt=X1+H/2.
1200 Yt=Y1+H/2.*K1
1210 Tempp=Temp+Cc*H/2.
1220 K2=FNValue(Xt.Yt.A.B.Time.K.Tstart.Tempp)

```

```

1230      Xt=Xi+H/2.
1240      Yt=Yi+(-.5+1./SQR(2.))*H*K1+(1.-1./SQR(2.))*H*K2
1250      K3=FNValue(Xt,Yt,A.B.Time.K.Tstart,Temp)
1260      Xt=Xi+H
1270      Yt=Yi-(1./SQR(2.))*H*K2+(1.+1./SQR(2.))*H*K3
1280      Temp=Temp+Cc*H
1290      K4=FNValue(Xt,Yt,A.B.Time.K.Tstart,Temp)
1300      V1=2.*(1.-1./SQR(2.))
1310      V2=2.*(1.+1./SQR(2.))
1320      Yi=Yi+H/6.*(K1+V1*K2+V2*K3+K4)
1330      SUBEND
1340      !
1350      !
1360      DEF FNValue(X,Y,A,B,Time,K,Tstart,Temp)
1370      COM Timechg0,Timechg1,Timechg2,Timechg3,Cc,A0
1380      COM Tg0temp,Tg0last,Tg0now,Alast,Anow
1390      COM Nn,N0,N1,N2,N3,Kn1,Kn2,Kn3,Kn4,Kn5,Kn6,Kn7,Kn8
1400      T0=Temp
1410      IF Time=0 THEN
1420          Nn=N0
1430          Tg0now=Y
1440          Tg0last=Y
1450          Alast=A0
1460          GOTO 1740
1470      ELSE
1480          GOTO 1490
1490      END IF
1500      IF Time<Timechg0 THEN
1510          Nn=N0*EXP((Time)*Kn2)
1520          GOTO 1740
1530      ELSE
1540          GOTO 1550
1550      END IF
1560          IF Time<Timechg1 THEN
1570              Nn=N1*EXP(Time*Kn4)
1580              GOTO 1740
1590          ELSE
1600              GOTO 1610
1610          END IF
1620          IF Time<Timechg2 THEN
1630              Nn=N2*EXP(Time*Kn6)
1640              GOTO 1740
1650          ELSE
1660              GOTO 1670
1670          END IF
1680          IF Time<Timechg3 THEN
1690              Nn=N3*EXP(Time*Kn8)
1700              GOTO 1740
1710          ELSE
1720              GOTO 1730
1730          END IF
1740      !
1750      Anow=Alast*(Tg0last/Tg0now)^Nn
1760      A=Anow
1770      B=B
1780      T1=A*(T0-Y)
1790      T2=B+T0-Y
1800      T3=T1/T2
1810      Value=K*EXP(T3)
1820      RETURN Value
1830      FNEND

```



```

1840      !
1850      !
1860  DEF FNVal0(A0,B0,Time0,Tg0,K,Temp1)
1870      A=A0
1880      B=B0
1890      T1=A*(Temp1-Tg0)
1900      T2=B+Temp1-Tg0
1910      T3=T1/T2
1920      Value1=K*EXP(T3)
1930      RETURN Value1
1940  FNEND
1950      !
1960      !

```

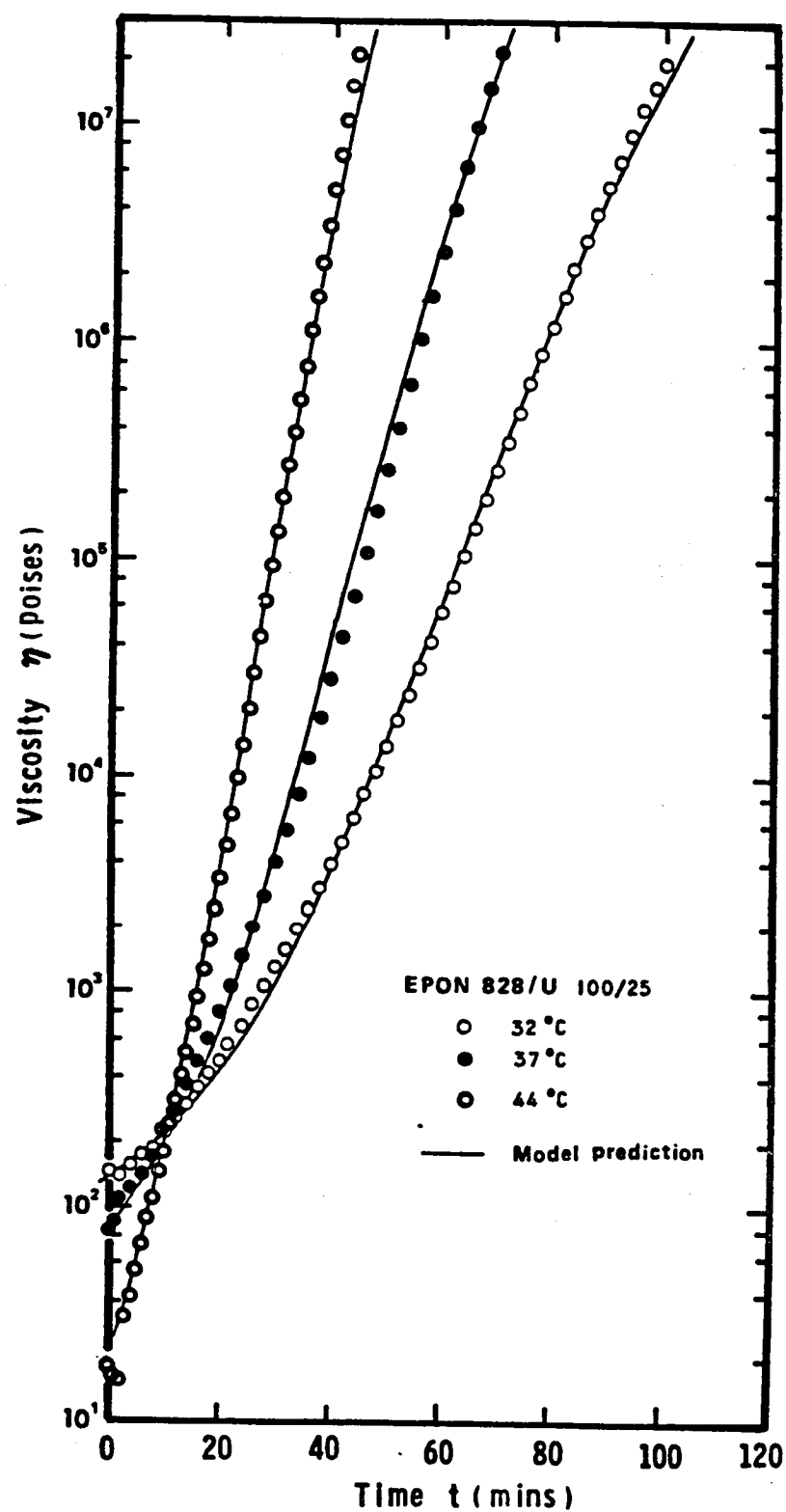


Figure 1. Comparisons between experimental chemoviscosity data and the model predictions for EPON 828 with Agent U. Chemoviscosity of the resin is measured by Rheometrics System 4 Rheometer under three isothermal curing conditions.

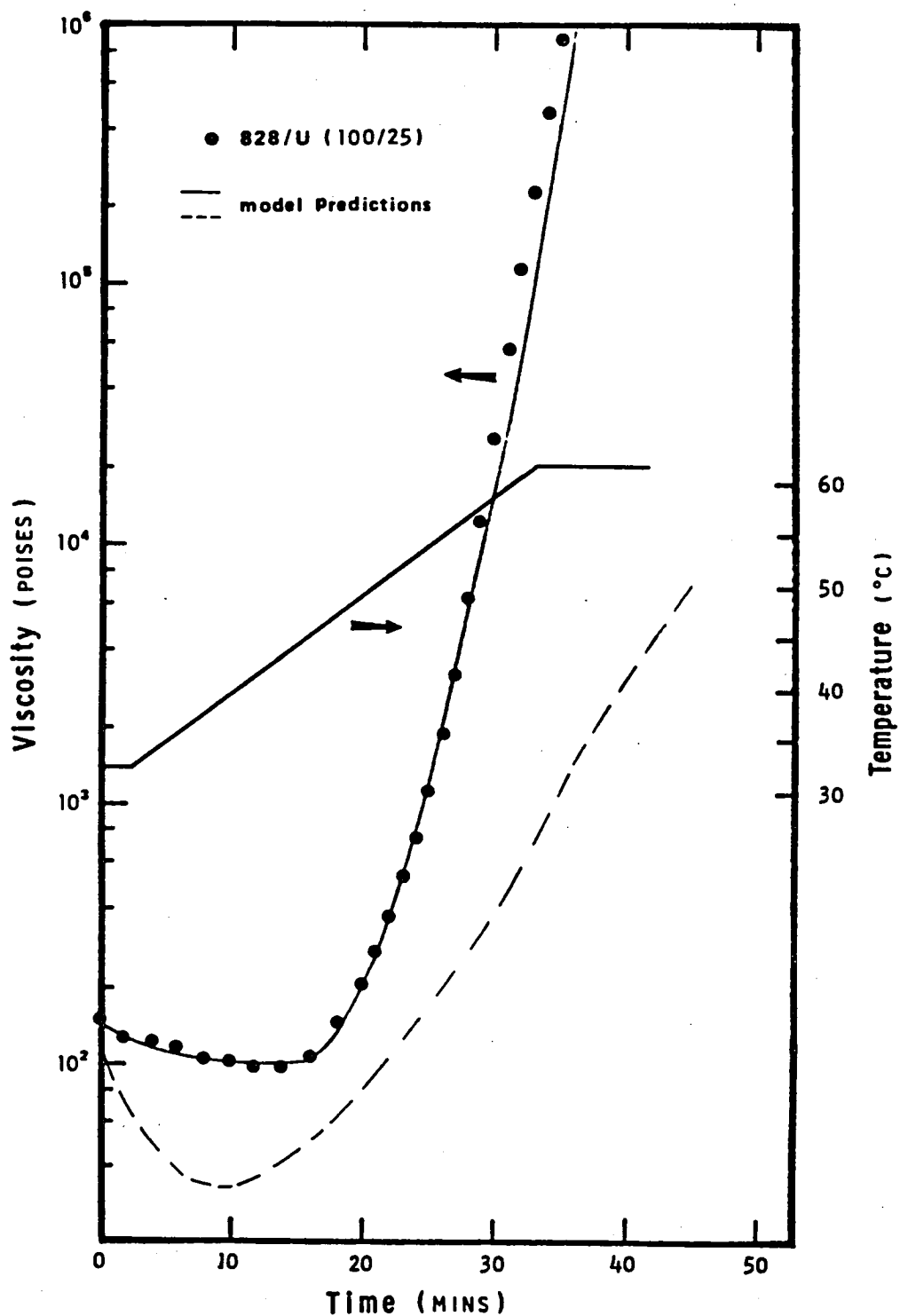


Figure 2. Comparisons between experimental non-isothermal chemoviscosity and the model predictions for EPON 828 with Agent U. Chemoviscosity of the resin is measured by Rheometrics System 4 Rheometer. The cure cycle (temperature profile) is also shown.²⁷

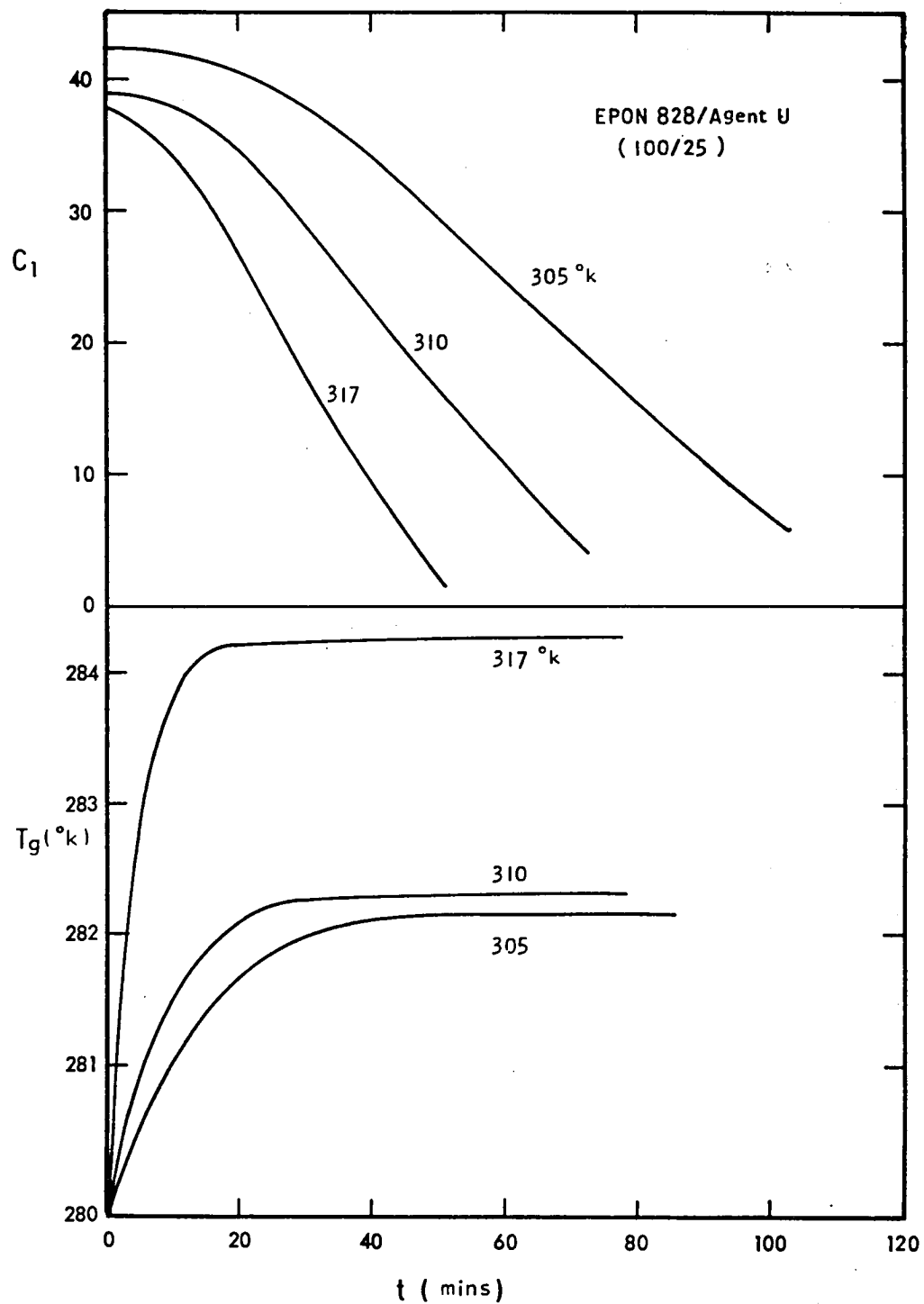


Figure 3. Variations of $T_g(t)$ and C_1 during cure obtained from the simulation models in Figure 1 for EPON 828/U resin system under isothermal curing conditions.

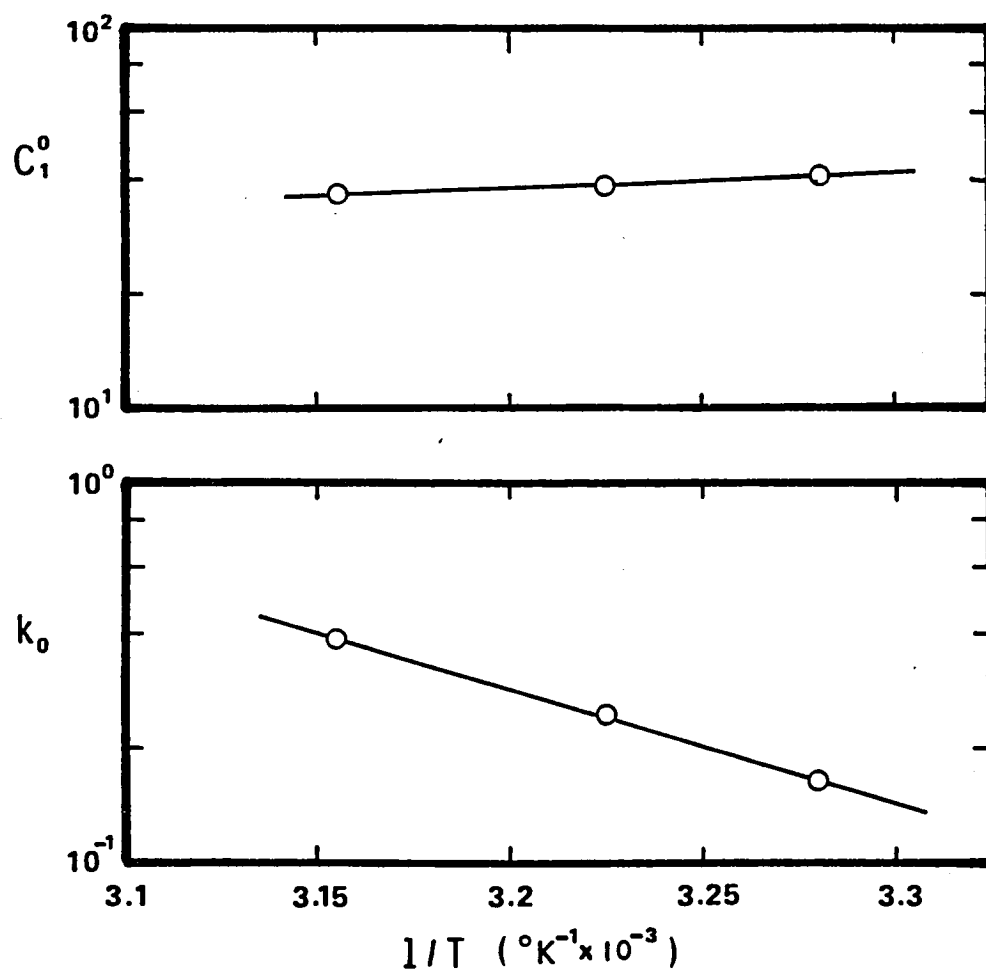


Figure 4. Arrhenius relationship for the model parameters.

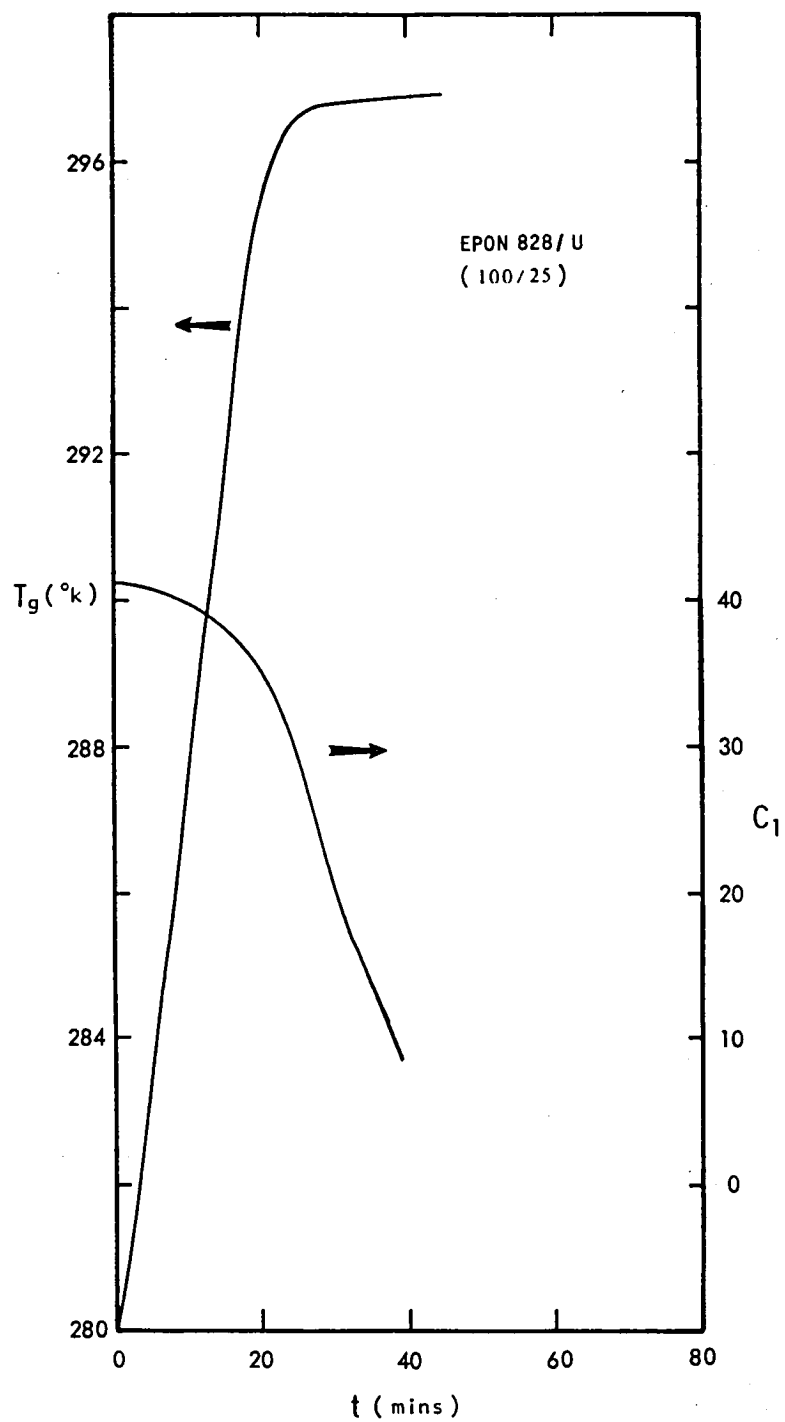


Figure 5. Variations of $T_g(t)$ and C_1 during cure obtained from the simulation model in Figure 2 for EPON 828/U resin system under dynamic heating conditions.

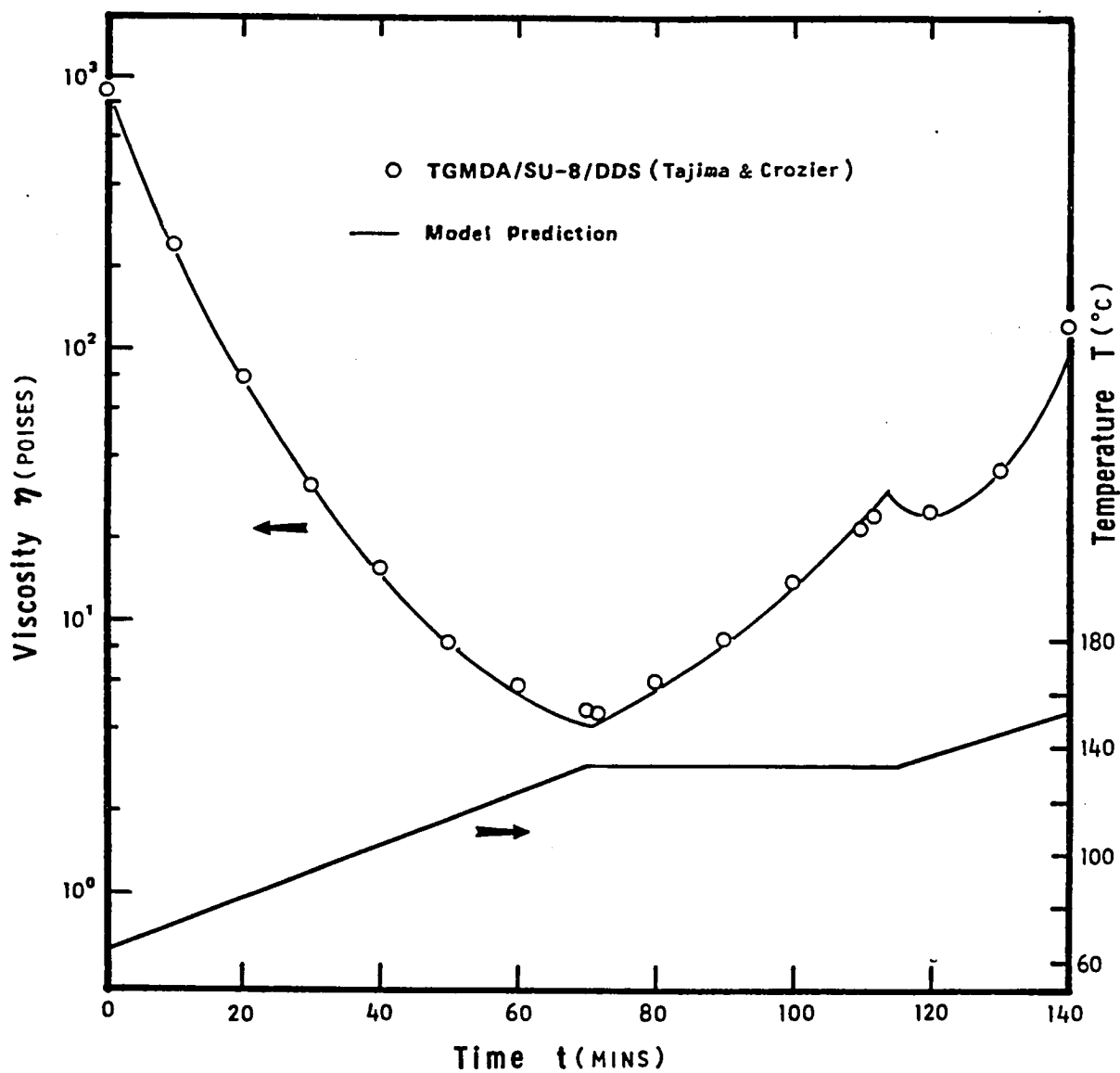


Figure 6. Comparisons between experimental non-isothermal chemoviscosity data and the model predictions. Cure cycle is also included. The data were reported by Tajima and Crozier for TGMDA-MY720/SU-8/DDS.

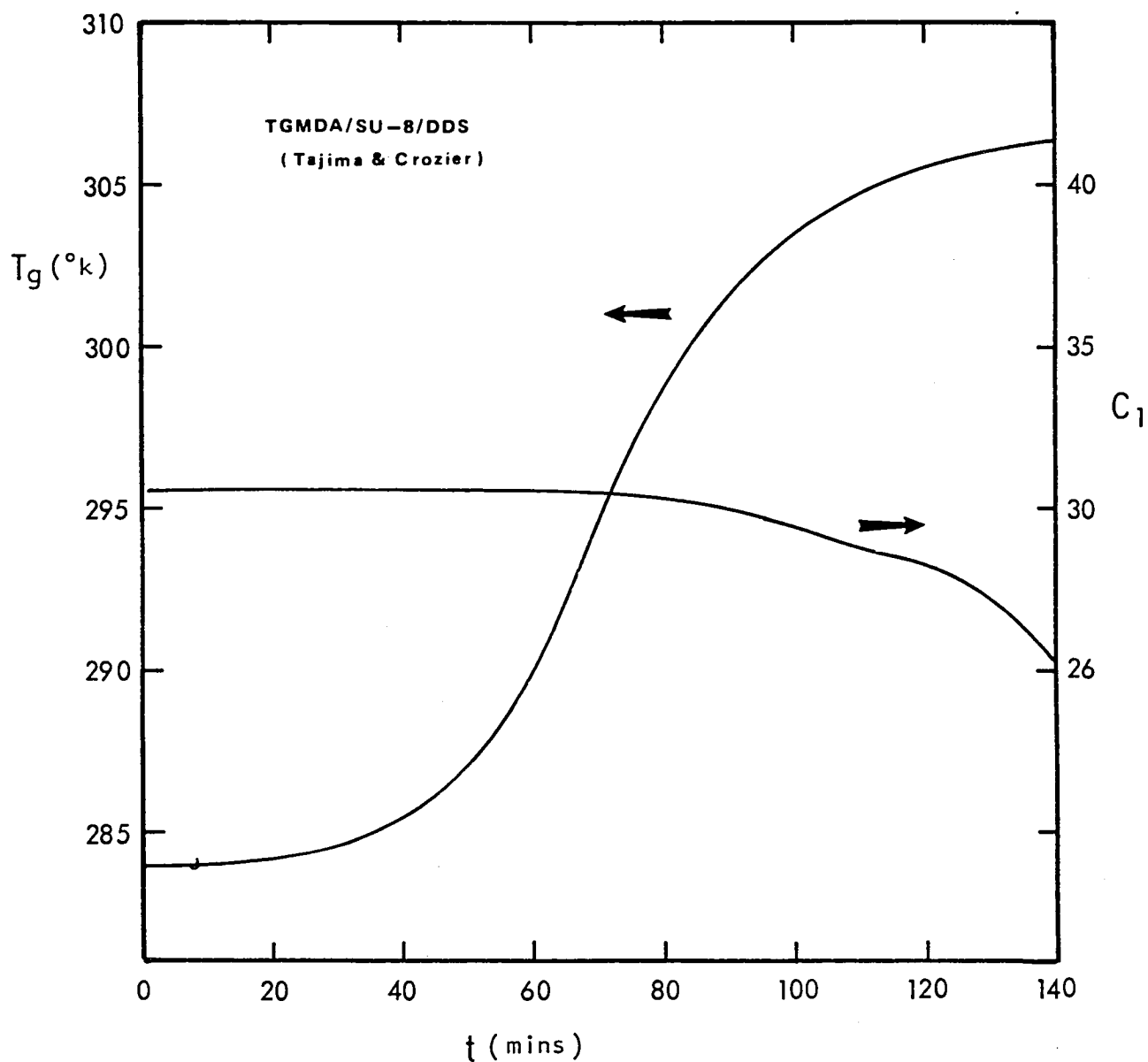


Figure 7. Variations of $T_g(t)$ and C_1 during cure obtained from the simulation model in Figure 6 for the TGMDA/SU-8/DDS resin system under dynamic heating conditions.

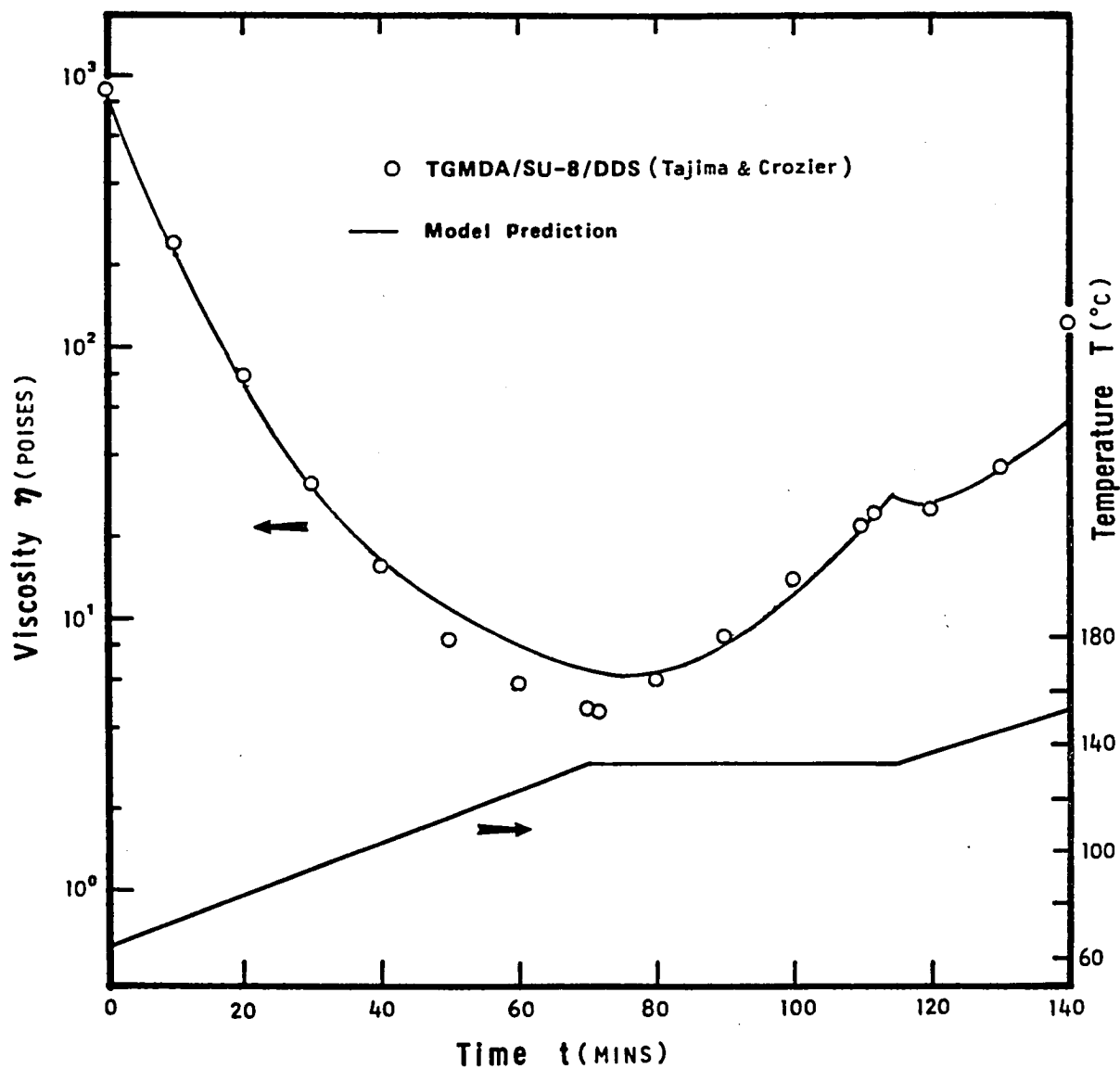


Figure 8. Same captions as in Figure 2, except that Eqs. (6a,b) are replaced by Eqs. (10a,b) to incorporate with the model Eq. (9).

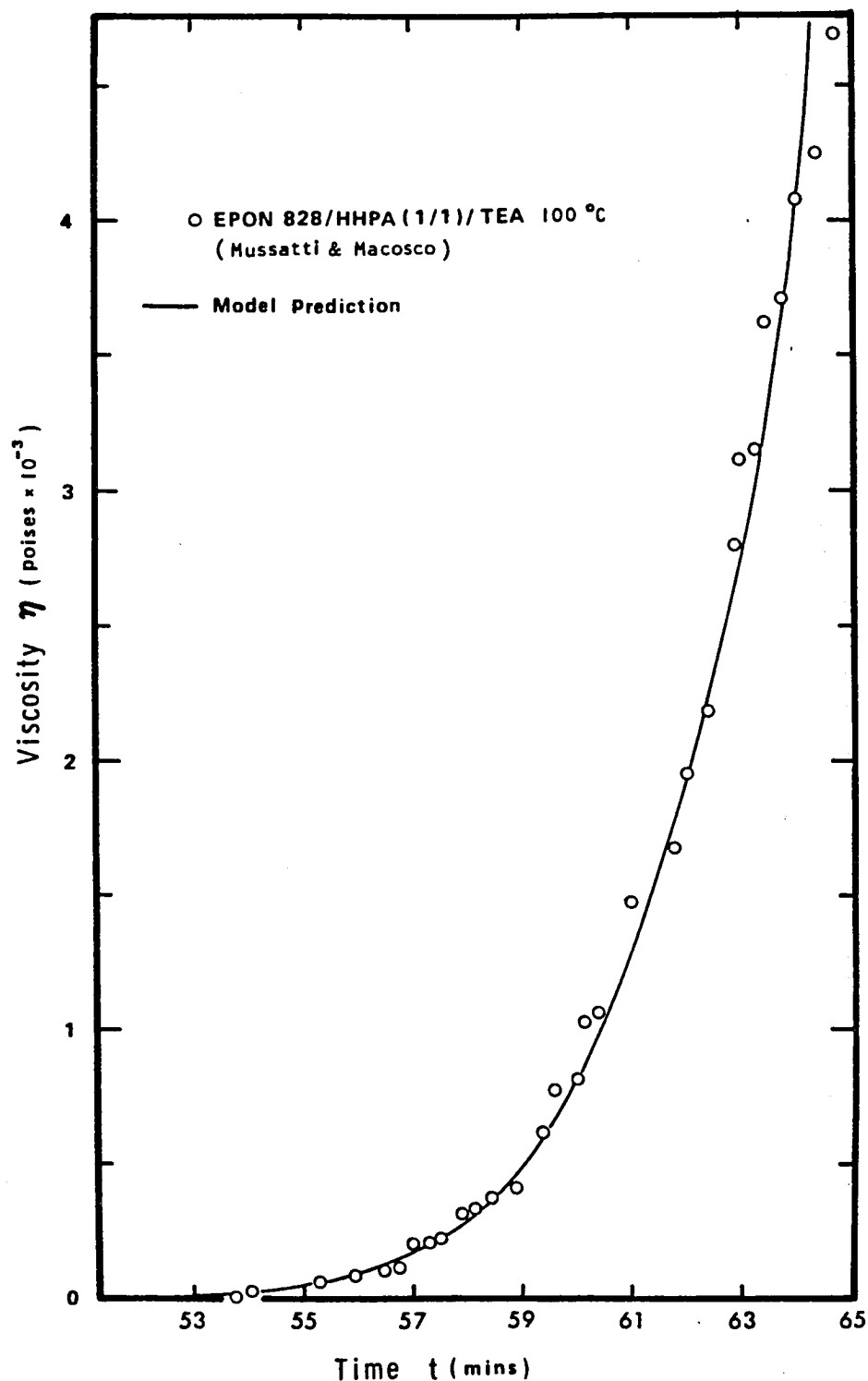


Figure 9. Comparisons between the experimental steady shear chemoviscosity data and the model predictions. Data were reported by Mussatti and Macosko for EPON 828/HHPA under isothermal curing at 100°C.

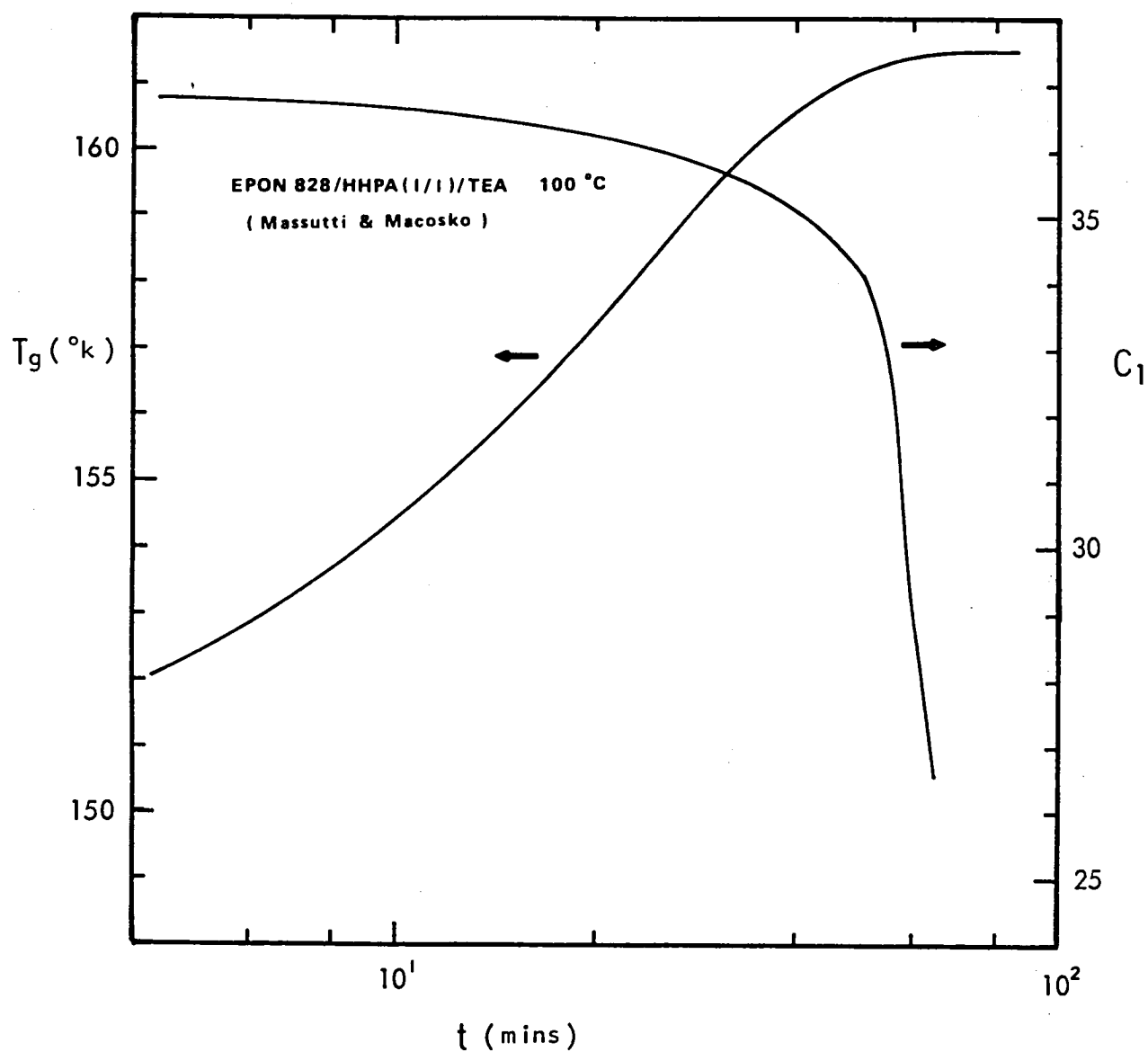


Figure 10. Variations of $T_g(t)$ and C_1 during cure obtained from the simulation model in Figure 9 for the EPON 828/HHPA/TEA resin system under isothermal cure conditions.

1. Report No. NASA CR-172443		2. Government Accession No.		3. Recipient's Catalog No.	
4. Title and Subtitle CHEMOVISCOSITY MODELING FOR THERMOSETTING RESINS - I				5. Report Date November 1984	
				6. Performing Organization Code	
7. Author(s) Tan-Hung Hou				8. Performing Organization Report No.	
9. Performing Organization Name and Address Kentron International, Inc. Aerospace Technologies Division 3221 N. Armistead Avenue Hampton, VA 23666				10. Work Unit No.	
				11. Contract or Grant No. NAS1-16000	
12. Sponsoring Agency Name and Address National Aeronautics and Space Administration Washington, DC 20546				13. Type of Report and Period Covered Contractor Report	
				14. Sponsoring Agency Code 505-33-33-01	
15. Supplementary Notes Langley Technical Monitor: R. M. Baucom Final Report					
16. Abstract A new analytical model for chemoviscosity variation during cure of thermosetting resins has been developed. This model is derived by modifying the widely used WLF (Williams-Landel-Ferry) Theory in polymer rheology. Major assumptions involved are that the rate of reaction is diffusion controlled and is linearly inversely proportional to the viscosity of the medium over the entire cure cycle. The resultant first order nonlinear differential equation is solved numerically, and the model predictions compare favorably with experimental data of EPON 828/Agent U obtained on a Rheometrics System 4 Rheometer. It has been shown that the model can describe chemoviscosity up to a range of six orders of magnitude under isothermal curing conditions. The extremely non-linear chemoviscosity profile for a dynamic heating cure cycle can be predicted as well. The model is also shown to predict changes of glass transition temperature for the thermosetting resin during cure. The physical significance of this prediction is unclear at the present time, however, and further research is required. From the chemoviscosity simulation point of view, the technique of establishing an analytical model as described here can easily be applied to any thermosetting resin. The model thus obtained can be used in real-time process controls for fabricating composite materials.					
17. Key Words (Suggested by Author(s)) Thermoset, Chemoviscosity, Autoclave, WLF theory, Thermoset curing			18. Distribution Statement Unclassified - Unlimited Subject Category 24		
19. Security Classif. (of this report) Unclassified	20. Security Classif. (of this page) Unclassified	21. No. of Pages 39	22. Price A03		

